Entire set of dynamical excitations of a one-dimensional Fulde-Ferrell-pairing Fermi superfluid based on momentum excitation

Peng Zou,[1] Huaisong Zhao,[1,*] Feng Yuan,[1,†] and Shi-Guo Peng[2,‡]

[1]*Centre for Theoretical and Computational Physics, College of Physics, Qingdao University, Qingdao 266071, China*

[2]*State Key Laboratory of Magnetic Resonance and Atomic and Molecular Physics, Innovation Academy for Precision Measurement Science and Technology, Chinese Academy of Sciences, Wuhan 430071, China*

(Received 4 January 2024; accepted 3 May 2024; published 20 May 2024)

We theoretically investigate a one-dimensional Fulde-Ferrell Fermi superfluid at a finite effective Zeeman field h and study all of the dynamical excitations related to density perturbation. By calculating the density dynamic structure factor, we find anisotropic dynamical excitations in both collective modes and single-particle excitations. Along the direction of center-of-mass momentum p, there are two obvious gapless collective modes with different speeds and two kinds of continuous regimes related to single-particle excitation. The lower collective modes are from the usual gauge symmetry breaking and have a larger speed than the one in the negative direction of p. The higher one is due to the direction spontaneous symmetry breaking of center-of-mass momentum p and separates a gapless lower-branch single-particle excitation from the other gapped higher-branch single-particle excitation in the positive p direction. However, this higher mode disappears in the opposite direction of p, where two single-particle excitations overlap with each other. These signals of dynamical excitations could help to distinguish a Fulde-Ferrell superfluid from the conventional Bardeen-Cooper-Schrieffer superfluid in future experiments.

DOI: 10.1103/PhysRevA.109.053313

I. INTRODUCTION

Since the discovery of superconducting phenomena in mercury by Onnes in 1911, it was realized that particles with opposite momentum and spin can generate a molecular Cooper pair carrying zero center-of-mass (c.m.) momentum p to decrease energy. This is explained by the Bardeen-Cooper-Schrieffer (BCS) theorem, and the forming superconductor (superfluid) state originates from the Bose-Einstein-Condensation (BEC) of Cooper pairs at zero momentum. Later, another kind of pairing mechanism was theoretically predicted by Fulde and Ferrel (FF) [1], and Larkin and Ovchinnikov (LO) [2], which introduces that Cooper pairs can also carry a finite c.m. momentum and condense at a nonzero momentum p with the order parameter in either a plane-wave FF type, $\Delta(\boldsymbol{r}) = \Delta e^{i\boldsymbol{p}\cdot\boldsymbol{r}}$, or a standing-wave LO type, $\Delta(\boldsymbol{r}) = \Delta\cos(\boldsymbol{p}\cdot\boldsymbol{r})$. In such an ansatz, these two mismatched Fermi surfaces of different spin components can overlap, thereby supporting a spatially inhomogeneous superfluidity. These pairing states generate an exotic Fulde-Ferrell-Larkin-Ovchinnikov (FFLO) superfluidity [3].

These FFLO superfluids have been actively searched for almost six decades. In condensed matter physics, some strong signals of FFLO states come from the research in heavy fermions [4–9] and organic superconductors [10], which are only indirect experimental evidence. Recently, several experimental works reported evidence of a pair-density wave in a high-T_c superconductor using the scanning tunneling microscopy technique [11–13], which renewed a strong interest in the topic and provides new possibilities to search and study the FFLO state. An ultracold atomic Fermi gas has proven to be an ideal tabletop system for the pursuit of FFLO superfluidity [14]. The FFLO state is thought to be very fragile in three dimensions and has quite narrow parameter space. Both the lower spatial dimension [15] and spin-orbit-coupling effect [16–20] in a Fermi superfluid have been reported to expand the parameter space of a FFLO state in the possible phase diagrams. Also, a theoretical strategy via a dark-state control of Feshbach resonance was proposed to realize a FF superfluid in ultracold atomic gases [21].

It is expected that the full dynamical excitations of a certain matter state can be utilized to check the existence of this state or distinguish it from other states. The dynamic structure factor is an important many-body physical quantity and includes rich information related to dynamical excitations of the system [22,23]. Experimentally, the dynamic structure factor can be directly measured by a two-photon Bragg scattering technique, which had been used to investigate dynamical excitations of the BCS-BEC crossover Fermi superfluid, including the single-particle excitations [24], collective Goldstone phonon mode [25], second sound [26], and Higgs mode [27]. A spin-charge separation of the repulsive one-dimensional (1D) Fermi gas has also been studied using this technique [28]. Some interesting spatial modulations of pair and spin correlation functions related to a 1D FFLO superfluid in a Tomonaga-Luttinger liquid were reported using a Bethe ansatz technique [29]. Thus it is interesting to study

*hszhao@qdu.edu.cn
†yuan@qdu.edu.cn
‡pengshiguo@wipm.ac.cn

the dynamical excitations of a FFLO Fermi superfluid and find its dynamical character related to its own symmetry structure.

In this paper, we theoretically investigate a 1D spin-polarized Fermi superfluid in an FF-type pairing state and discuss its entire dynamical excitations by numerically calculating the dynamic structure factor of this system with the random phase approximation (RPA) [30,31]. The main idea of this theoretical strategy is to get the state of equation of the system in the level of mean-field theory, while the prediction of the dynamical response is beyond mean-field theory due to the proper treatment of the fluctuation term in the Hamiltonian using RPA [32]. In a three-dimensional BCS-BEC crossover Fermi superfluid, the prediction about dynamical excitations from this method even quantitatively agrees well with that from experiments [33–35] and the two-dimensional theoretical results of this method qualitatively agree with quantum Monte Carlo data [36]. So it is reasonable to expect that this method can provide a qualitatively accurate prediction of dynamical excitations in a 1D system. We will initially discuss the state of equation of the system in a FF superfluid and then introduce all possible dynamical excitations, which may provide some background knowledge to the anisotropic Josephson effect related to the FFLO state.

This paper is organized as follows. In the next section, we use the motion equation of the Green' s function to introduce the microscopic model of a 1D spin-polarized interacting Fermi gas and outline the mean-field approximation, and then show how to calculate the response function with RPA. We give results of the dynamic structure factor of FF superfluids in Sec. III, and we give our conclusions and outlook in Sec. IV. Some calculation details are listed in the Appendix.

II. METHODS

A. Model and Hamiltonian

We consider uniform 1D spin-polarized Fermi gases with s-wave contact interaction. The system can be described by a model Hamiltonian,

$$H = \sum_{k\sigma}(\epsilon_k - \mu_\sigma)c^\dagger_{k\sigma}c_{k\sigma} + g_{1D}\sum_{pkk'}c^\dagger_{k\uparrow}c^\dagger_{p-k\downarrow}c_{p-k'\downarrow}c_{k'\uparrow}, \quad (1)$$

where $\epsilon_k = k^2/2m$ is the dispersion relation of spin-σ free particles with mass m in reference to the chemical potential μ_σ, and $c_{k\sigma}(c^\dagger_{k\sigma})$ is their annihilation (generation) operator in momentum representation. Here and in the following, we have set physical quantities $\hbar = k_B = 1$ for convenience. The 1D interaction $g_{1D} = -\gamma n_0/m$ describes an attractive interplay between opposite spin components with a dimensionless strength γ. Since we consider a uniform system with bulk density n_0, the inverse of Fermi wave vector $k_F = \pi n_0/2$ and Fermi energy $E_F = k_F^2/2m$ are used as length and energy units, respectively. Usually, the difference of the chemical potential is used to define an effective Zeeman field $h = (\mu_\uparrow - \mu_\downarrow)/2$, and $\mu = (\mu_\uparrow + \mu_\downarrow)/2$ is the average chemical potential.

At zero temperature $T = 0$, usually the system will come into a superfluid state in which two opposite-spin atoms form a molecular Cooper pair. Interestingly, an FF-type superfluid, whose Cooper pairs have a nonzero c.m. momentum p, possibly becomes the ground state at a nonzero effective Zeeman field h. In a standard mean-field treatment, the order parameter of the FF superfluid can be expressed in a plane-wave form, $\Delta(x) \equiv \Delta e^{ipx}$, where the c.m. momentum p and pairing gap $\Delta = g_{1D}\sum_k\langle c_{-k+p/2\downarrow}c_{k+p/2\uparrow}\rangle$ are two important degrees of freedom of the order parameter $\Delta(x)$. Within this approximation, a mean-field Hamiltonian is expressed as

$$H_{\rm mf} = \sum_k(\xi_k - h\sigma_z)c^\dagger_{k\sigma}c_{k\sigma} - \Delta^2/g_{1D} - \sum_k\Delta(c_{-k+p/2\downarrow}c_{k+p/2\uparrow} + \text{H.c.}), \quad (2)$$

where $\xi_k = \epsilon_k - \mu$. The exact solution of mean-field Hamiltonian $H_{\rm mf}$ can be obtained by the motion equation of Green's functions. Finally, we get three independent Green's functions, whose expressions are

$$G_1 \equiv \langle\langle c_{k+p/2\uparrow}|c^\dagger_{k+p/2\uparrow}\rangle\rangle = \sum_l\frac{[G_1]^l_k}{\omega - E^l_k}, \quad (3)$$

$$G_{2R} \equiv \langle\langle c^\dagger_{-k+p/2\downarrow}|c_{-k+p/2\downarrow}\rangle\rangle = \sum_l\frac{[G_{2R}]^l_k}{\omega - E^l_k}, \quad (4)$$

$$\Gamma \equiv \langle\langle c_{k+p/2\uparrow}|c_{-k+p/2\downarrow}\rangle\rangle = \sum_l\frac{[\Gamma]^l_k}{\omega - E^l_k}. \quad (5)$$

The double angular brackets in the above equations are used to define the Fourier transformation of the double-time Green's function. Here it should be emphasized that the expression of spin-down Green's function G_{2R} is different from the one of spin-up Green's function G_1. Their definitions closely depend on the way they are coupled to pairing Green's function Γ when solving the motion equation of the Green's function. All of the expressions of $[G_1]^l_k$, $[G_{2R}]^l_k$, and $[\Gamma]^l_k$ will be listed in the Appendix. $l = 1, 2$ denotes two branches of quasiparticle energy spectrum $E^{(1)}_k$ and $E^{(2)}_k$,

$$E^{(1,2)}_k = \frac{kp}{2m} - h \pm E_k, \quad (6)$$

where $E_k = \sqrt{\xi^2_{kp} + \Delta^2}$ and $\xi_{kp} = \epsilon_k + \epsilon_p/4 - \mu$. In the typical parameters used in this paper, we find that the value of $E^{(2)}_k$ is always negative, while $E^{(1)}_k$ can be either positive or negative. The distributions of these two spectra are shown in Fig. 1, in which $E^{(1)}_k$ is negative when $-2.17k_F < k < 0.12k_F$.

The mean-field thermodynamic potential of the system reads

$$\Omega = -\Delta^2/g_{1D} + \sum_k(\xi_k - E_k) + \sum_k T\left[\ln f\left(-\mathrm{E}^{(1)}_k\right) + \ln f\left(\mathrm{E}^{(2)}_k\right)\right], \quad (7)$$

which is connected to the free energy by $F = \Omega + \mu N$. Here, $f(x) = 1/(e^{x/T} + 1)$ is the Fermi-Dirac distribution function at temperature T. In this paper, we focus our discussion on an almost zero temperature ($T = 0.01T_F$) to avoid an unnecessary numerical divergence induced by zeros of $E^{(1)}_k$.

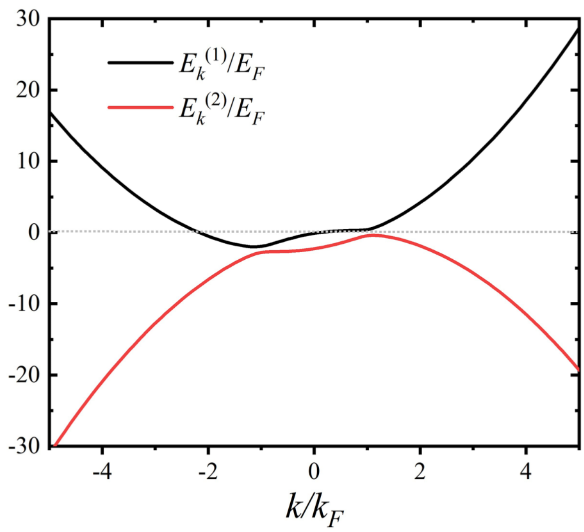

FIG. 1. Two branches of a single-particle excitation spectrum at interaction strength $\gamma = 3$ and effective Zeeman field $h = 1.2E_F$. Here, the c.m. momentum $p = 1.18k_F$.

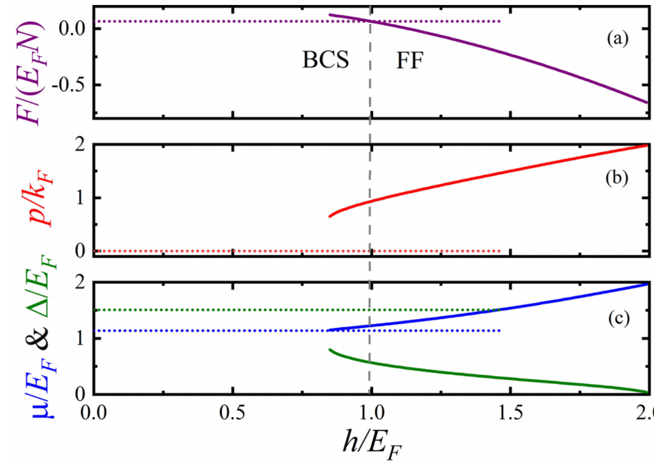

FIG. 2. State of equation at interaction strength $\gamma = 3$. The panels show the curves of (a) free energy, (b) c.m. momentum, and (c) average chemical potential and order parameter at different effective Zeeman fields, respectively.

B. State of equations

The values for average chemical potential μ, amplitude of order parameter Δ, and c.m. momentum p can be, respectively, determined with minimization of thermodynamic potential Ω in Eq. (7), namely, $N = -\partial\Omega/\partial\mu$, $\partial\Omega/\partial\Delta = 0$, and $\partial\Omega/\partial p = 0$. These three relations, respectively, give the total particle number equation,

$$N = \sum_k \left(1 - \frac{\xi_{kp}}{E_k}\right) + \sum_k \frac{\xi_{kp}}{E_k}\left[f\left(E_k^{(1)}\right) + f\left(-E_k^{(2)}\right)\right], \quad (8)$$

pairing gap equation,

$$\frac{\Delta}{g_{1D}} = \sum_k \frac{\Delta}{2E_k}\left[f\left(E_k^{(1)}\right) + f\left(-E_k^{(2)}\right) - 1\right], \quad (9)$$

and c.m. momentum equation,

$$\sum_k \left[p\left(1 - \frac{\xi_{kp}}{E_k}\right) + \left(2k + \frac{\xi_{kp}}{E_k}p\right) f\left(E_k^{(1)}\right) - \left(2k - \frac{\xi_{kp}}{E_k}p\right) f\left(-E_k^{(2)}\right)\right] = 0. \quad (10)$$

The values of μ, Δ, and p should be self-consistently solved with Eqs. (8)–(10).

All possible stable states of a system are determined with all minima in free energy F. Generally, there are three possible states here. Besides the trivial normal state, which always has a zero pairing gap Δ and the largest free energy, the conventional BCS superfluid and FF superfluid are the other two states with relatively lower free energy. As shown in Fig. 2, at a small h, the conventional BCS superfluid is the ground state of the system, whose c.m. momentum $p = 0$ all the time. The value of h can hardly influence the chemical potential μ and pairing gap Δ, which can be thought of as the analogy of the Meissner effect in the superfluid. Interestingly, an FF superfluid with a nonzero c.m. momentum p begins to turn out when h is large enough, whose free energy is larger than that of the BCS superfluid. When h arrives at a critical value h_c (whose value is a little smaller than $1.0E_F$), this FF superfluid shares the same free energy as the BCS superfluid. Further increasing h, the FF superfluid replaces the BCS superfluid to be the new ground state of the system for $h > h_c$. This phase transition was introduced in Ref. [15]. Here, Δ and p are two necessary degrees of freedom in a FF-type order parameter, $\Delta(x) = \Delta e^{ipx}$. Pairing gap Δ is related to the conventional gauge symmetry breaking of superfluidity, and the direction of c.m. momentum p is related to another spontaneous symmetry breaking since $\pm p$ corresponds to the same free energy. While Δ always decreases with h, p shows a monotonically increasing behavior with h. The different dependence behavior of Δ and p with effective Zeeman field h reflects that they come from different symmetry breaking and may induce different collective modes. We have to emphasize that the phase transition predicted by mean-field theory is a first-order one, different from the continuous transition given by a better method such as bosonization [37]. Clearly, this is the defect of mean-field theory in predicting the state of equation. However, both methods qualitatively admit the existence of the FFLO state, which builds a foundation to ensure the qualitative correctness of the background matter state. We also check that the same phase transition also happens at different interaction strengths γ with different critical Zeeman fields h_c, whose value is shown in Fig. 3. A larger interaction strength γ requires a bigger critical effective Zeeman field h_c to make the system come into the FF superfluid state.

C. Calculation of dynamical excitations

In this section, we will introduce the main idea of RPA, which is a beyond-mean-field strategy of treating the fluctuation part in the Hamiltonian to investigate dynamical excitations.

When an interacting system comes into a superfluid state, usually there will be four typical densities. Besides the normal spin-up density $n_1 = \langle\psi_\uparrow^\dagger\psi_\uparrow\rangle$ and spin-down density

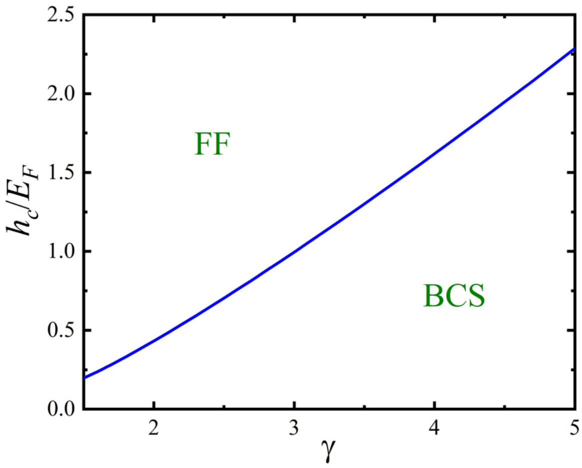

FIG. 3. The critical effective Zeeman field h_c at different interaction strengths γ.

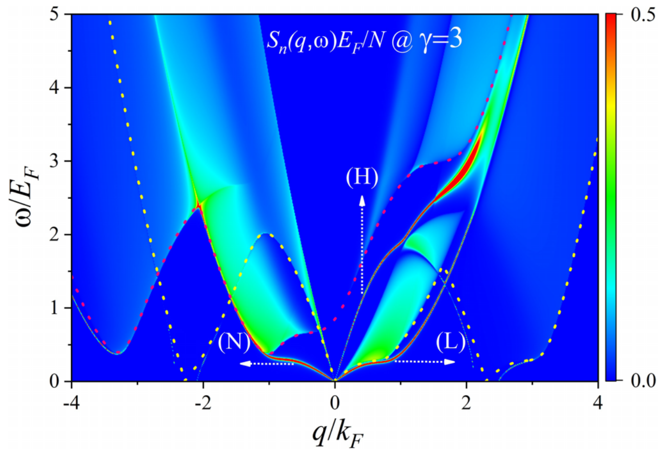

FIG. 4. The density dynamic structure factor $S_n(q,\omega)$ of the FF superfluid at interacting strength $\gamma = 3$. L: the lower collective phonon mode along the c.m. momentum p direction; H: the higher collective phonon mode; N: the collective phonon mode along the opposite direction of p.

$n_2 = \langle\psi_\downarrow^\dagger\psi_\downarrow\rangle$, the pairing physics of opposite-spin atoms generates the other anomalous density $n_3 = \langle\psi_\downarrow\psi_\uparrow\rangle$ and its conjugate counterpart $n_4 = \langle\psi_\uparrow^\dagger\psi_\downarrow^\dagger\rangle$. These anomalous densities describe phase-coherent Cooper pairs with zero or finite c.m. momentum p. The interaction between particles makes these four densities couple closely with each other. Any fluctuation in each kind of density will influence other densities and generate an obvious density fluctuation of them. In the frame of linear response theory, any weak perturbation potential $V_{\rm pert}$ will induce density fluctuation δn, which is connected to $V_{\rm pert}$ by response function χ, namely, $\delta n = \chi V_{\rm pert}$.

The entire dynamical excitations of the system consist of possible collective excitations and single-particle excitations, which are also closely connected to the physical properties of the Cooper pairs. Their spontaneously breaking phase generates a gapless Goldstone collective mode, while the breaking of the Cooper pairs forms parts of the single-particle excitation. These dynamical excitations can be well described by the density dynamic structure factor, which is from the imaginary part of the related response functions χ.

The direct calculation of the dynamic structure factor suffers from the many-body difficulty. A feasible approximation to overcome this problem is from RPA, which is first introduced by Anderson and has be verified to be a reliable way to study dynamical excitations [33,34]. In our previous work, we introduced how to calculate the dynamic structure factor with RPA [38,39]. This approximation finds the connection between the beyond-mean-field response function χ and its mean-field approximation χ^0 by the following equation:

$$\chi = \frac{\chi^0}{1 - \chi^0 M_I g_{1\rm D}}. \tag{11}$$

Here, the constant matrix $M_I = \sigma_0 \otimes \sigma_x$ is the direct product between unit matrix σ_0 and Pauli matrix σ_x, reflecting the coupling situation of four types of densities. χ^0 is a four-dimensional matrix in the mean-field level, and its ij matrix element $\chi_{ij}^0 \equiv -\langle\hat{n}_i\hat{n}_j\rangle$ reflects the interaction-induced coupling between density n_i and n_j. When the system comes into the FF superfluid, the symmetry properties of the system induce that the mean-field response function matrix χ^0 only has nine independent matrix elements, namely,

$$\chi^0 = \begin{bmatrix} \chi_{11}^0 & \chi_{12}^0 & \chi_{13}^0 & \chi_{14}^0 \\ \chi_{12}^0 & \chi_{22}^0 & \chi_{23}^0 & \chi_{24}^0 \\ \chi_{14}^0 & \chi_{24}^0 & -\chi_{12}^0 & \chi_{34}^0 \\ \chi_{13}^0 & \chi_{23}^0 & \chi_{43}^0 & -\chi_{12}^0 \end{bmatrix}, \tag{12}$$

where $\chi_{12}^0 = \chi_{21}^0 = -\chi_{33}^0 = -\chi_{44}^0$, $\chi_{31}^0 = \chi_{14}^0$, $\chi_{32}^0 = \chi_{24}^0$, $\chi_{41}^0 = \chi_{13}^0$, and $\chi_{42}^0 = \chi_{23}^0$. After Fourier transformation to the above response function matrix elements, we obtain the expression of all matrix elements in the momentum-energy representation.

With Eqs. (11) and (12), we can obtain the expression of the total-density response function, $\chi_n \equiv \chi_{11} + \chi_{22} + \chi_{12} + \chi_{21}$. Based on the fluctuation and dissipation theorem, the imaginary part of χ_n is connected to the density dynamical structure factor by

$$S_n = -\frac{1}{\pi}\frac{1}{1 - e^{-\omega/T}}{\rm Im}(\chi_n). \tag{13}$$

III. RESULTS

We numerically calculate the density dynamic structure factor $S_n(q,\omega)$ of a FF superfluid at interaction strength $\gamma = 3$. We choose the direction of c.m. momentum p along the positive direction of transferred momentum q. The results are shown in Fig. 4. Intuitively, we see an anisotropic dynamical behavior. The dynamical excitation at a positive transferred momentum q is different from the one at a negative q. This is due to the direction dependence of the nonzero c.m. momentum p in the FF superfluid. Along the direction of c.m. momentum p (namely, $q > 0$), we see two kinds of gapless collective mode [curves marked by (L) and (H)] and two separated regimes of single-particle excitation. When $q < 0$, the higher gapless collective mode disappears, and two kinds of single-particle excitation overlap with each other. The speed of the gapless collective phonon mode [curve marked by (N)] is a little smaller than that in the positive direction. In the following, we will separately introduce collective modes and single-particle excitations.

A. Collective modes

The origin of the collective mode is closely related to the symmetry breaking of a certain matter state. Usually, a gapless collective excitation comes from a certain spontaneous continuous symmetry breaking of the system. It is interesting to notice that there are two gapless collective modes at a positive transferred momentum q, which are also displayed in Fig. 4. The lower mode is the conventional collective Goldstone phonon mode [marked by (L)], which requires the lowest excitation energy among all possible excitations. It is due to the gauge symmetry breaking of order parameter $\Delta(x)$. As to the physical origin of the higher gapless collective mode [marked by (H)], we argue that it is due to the symmetry breaking of the direction of c.m. momentum p, which is continuous symmetry breaking in a higher-dimension system, but not continuous in a 1D system due to its specific spatial dimension. A similar higher mode is also reported in a lattice system in Refs. [40,41], and Ref. [41] explained it as a collective-type response of quasiparticles. Also, another similar mode as the higher collective one here is reported in a LO-type superconductor with order parameter $\Delta(x) = \Delta\cos(px)$, which is called the gapless Higgs mode since its amplitude of order parameter displays spatial periodic variation [42,43]. However, it is easy to know that the FF superfluid has a plane-wave order parameter $\Delta(x) = \Delta\exp(ipx)$, whose amplitude is always a constant value and keeps the continuous translational symmetry. Although the higher collective mode in the FF superfluid is gapless, it should come from a different symmetry-breaking physics from the one in the LO case. We argue that it comes from the direction symmetry breaking of c.m. momentum p since the velocity v_H of the higher mode shares the same effective Zeeman field h dependence as c.m. momentum p, which can be seen in both Figs. 2(b) and 5. This direction symmetry breaking of a 1D system here can be approximately thought to be a quasicontinuous one due to the specific dimension effect of the 1D system. Also, there is no Brillouin zone structure generated by continuous translational symmetry breaking in a plane-wave-type FF superfluid, and thus no gapless roton mode happens at a nonzero transferred momentum [44,45].

The other difference from the BCS superfluid is that the lowest collective phonon mode displays an anisotropic excitation between the positive and negative directions, which is due to the direction dependence of c.m. momentum p in the FF superfluid. A similar anisotropic dynamics of the phonon mode is also reported in a spin-polarized FFLO superfluid in a square optical lattice [41]. From Fig. 5, it is easy to know that the velocity v_N of the phonon mode in a negative p direction [marked by (N)] is always smaller than v_L in the positive q direction. Also, the absolute value of the phonon velocity decreases with h in the negative q direction.

The effective Zeeman field h dependence of the speed for three collective modes is shown in Fig. 5, which displays that both v_L and v_N decrease with h and slowly go to zero at a large enough h. Finally, Δ also touches zero and the superfluid

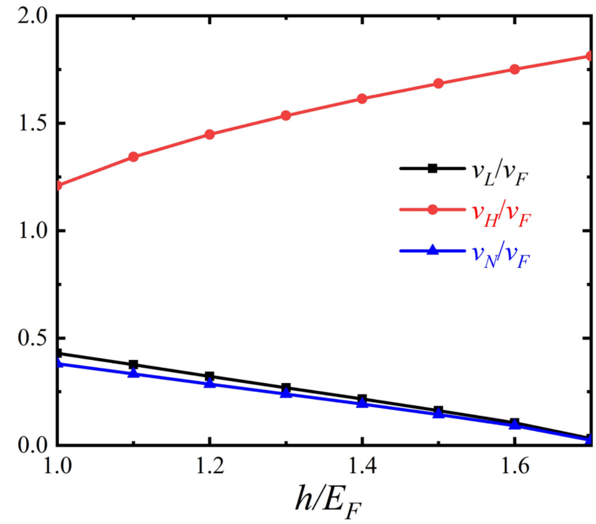

FIG. 5. Speeds of three collective modes at different effective Zeeman field h. v_L and v_H are, respectively, the speed of the lower and higher branch collective mode along the direction of c.m. momentum p, while v_N is the speed of the collective phonon mode in the opposite direction of p.

disappears when h is around $2.0E_F$. However, v_H always rises with h and this behavior is consistent with that of c.m. momentum p [Fig. 2(b)]. The similar h dependence between v_H and p again demonstrates a close connection between them. Also, the different h dependence between v_L and v_H demonstrates that the two gapless collective modes come from a different symmetry-breaking mechanism, and are related to a different fluctuation of the order parameter.

B. Single-particle excitations

Now we discuss the pair-breaking excitation, which is an important part of single-particle excitation and takes up large regimes in Fig. 4. This excitation is usually a continuous excitation and its lowest excitation energy is determined by the single-particle spectrum [Eq. (6)]. To understand all possible ways of pair-breaking excitation, it is better to understand this physics using part of the expression in the response function χ^0, namely,

$$\frac{f\left(E_p^l\right) - f\left(E_{p+q}^{l'}\right)}{i\omega_n + E_p^l - E_{p+q}^{l'}}. \tag{14}$$

Here, E_p^l should consider all possible combinations of the single-particle spectrum. As shown in Fig. 1, $E_k^{(2)}$ is always negative, and $E_k^{(1)}$ is positive except in a narrow regime $-2.17k_F < k < 0.12k_F$. The occurrence of one pair-breaking excitation requires that the numerator of Eq. (14) cannot be zero, and also $E_p^l - E_{p+q}^{l'} < 0$ to ensure a positive excitation energy.

Finally, we find two possible pair-breaking excitations, namely, $|E_k^{(1)} - E_{k+q}^{(1)}|$ (11-type excitation) at a limited regime of momentum k and $|E_k^{(2)} - E_{k+q}^{(1)}|$ (21-type excitation) at a full regime of k. And their minima are the lowest energy to break an FF-type Cooper pair, which are labeled by pink and yellow dotted lines in Fig. 4, respectively. These is no obvious

22-type excitation at zero temperature since the numerator of Eq. (14) is zero.

It should be emphasized that the 11-type excitations (dotted yellow line) are a gapless pair-breaking excitation and are absent in the conventional BCS superfluid. As also shown in Fig. 4, this gapless 11-type single-particle excitation is quite close to the lower collective mode in the positive q direction, and is well separated from the lower collective mode in the negative q direction. Physically, we guess this 11-type excitation is possibly the counterpart of the collective-type response of quasiparticles mentioned in Ref. [41]. Clearly, there is a slight bias between the predictions from the yellow dotted lines and the RPA prediction when q is around $\pm 2.5k_F$, which may be due to the limited excitation regime of momentum k in the 11-type excitation. The minimum of the 21-type excitation is labeled with a dotted pink line, and the 21-type single-particle excitation is always a gapped excitation. For a positive transferred momentum q, these two pair-breaking excitations are separated from each other by just the higher gapless collective mode. However, they are mixed with each other in a negative transferred momentum q. These differences can help one to find the higher collective mode in future experiments and distinguish a FF-type superfluid from a BCS superfluid.

IV. CONCLUSIONS AND OUTLOOK

In summary, we theoretically calculate the dynamic structure factor of a 1D FF superfluid with random phase approximation to study dynamical excitations. We find an anisotropic dynamical excitation between positive and negative directions in both collective modes and single-particle excitations. In the positive direction, we find two gapless collective modes. The lower one comes from the spontaneous breaking of gauge symmetry, while the higher one may come from the direction symmetry breaking of c.m. momentum p. The sound speed in the positive direction is larger than the one in the negative direction. There are two types of pair-breaking excitations, and one of them is a gapless excitation, which is absent in the BCS superfluid. In the positive direction, these two kinds of pair-breaking excitations are just separated by the higher gapless collective mode, but overlap with each other in the negative direction. These dynamical excitations could help to distinguish a FF superfluid from the conventional BCS superfluid in future experiments.

ACKNOWLEDGMENTS

We are grateful for discussions with Wei Yi, Xiaoquan Yu, and Hui Hu. This research is supported by National Natural Science Foundation of China under Grants No. U23A2073 (P.Z.), No. 11547034 (H.Z.), and No. 12374250 (S.-G.P.), and the National Key R&D Program under Grant No. 2022YFA1404102 (S.-G.P.).

APPENDIX: EXPRESSIONS OF GREEN'S FUNCTIONS AND RESPONSE FUNCTIONS

In this Appendix, we list the expressions of three Green's functions and mean-field response function χ^0. The first Green's function is $G_1(k,\omega)=\sum_l [G_1]_k^l/(\omega-E_k^l)$, with

$$[G_1]_k^{(1)}=\frac{E_k^{(1)}+\xi_{k-p/2}+h}{E_k^{(1)}-E_k^{(2)}},\quad [G_1]_k^{(2)}=-\frac{E_k^{(2)}+\xi_{k-p/2}+h}{E_k^{(1)}-E_k^{(2)}}.$$

The second one is $G_{2R}(k,\omega)=\sum_l [G_{2R}]_k^l/(\omega-E_k^l)$, with

$$[G_{2R}]_k^{(1)}=\frac{E_k^{(1)}-\xi_{k+p/2}+h}{E_k^{(1)}-E_k^{(2)}},\quad [G_{2R}]_k^{(2)}=-\frac{E_k^{(2)}-\xi_{k+p/2}+h}{E_k^{(1)}-E_k^{(2)}}.$$

The third Green's function is $\Gamma(k,\omega)=\sum_l [\Gamma]_k^l/(\omega-E_k^l)$, with

$$[\Gamma]_k^{(1)}=-\frac{\Delta}{E_k^{(1)}-E_k^{(2)}},\quad [\Gamma]_k^{(2)}=\frac{\Delta}{E_k^{(1)}-E_k^{(2)}}.$$

The expressions of all nine independent matrix elements in the mean-field response function χ^0 are, respectively,

$$\chi_{11}^0=+\sum_{pll'}[G_1]_p^l[G_1]_{p+q}^{l'}\frac{f(E_p^l)-f(E_{p+q}^{l'})}{i\omega_n+E_p^l-E_{p+q}^{l'}},$$

$$\chi_{12}^0=-\sum_{pll'}[\Gamma]_p^l[\Gamma]_{p+q}^{l'}\frac{f(E_p^l)-f(E_{p+q}^{l'})}{i\omega_n+E_p^l-E_{p+q}^{l'}},$$

$$\chi_{13}^0=+\sum_{pll'}[G_1]_p^l[\Gamma]_{p+q}^{l'}\frac{f(E_p^l)-f(E_{p+q}^{l'})}{i\omega_n+E_p^l-E_{p+q}^{l'}},$$

$$\chi_{14}^0=+\sum_{pll'}[\Gamma]_p^l[G_1]_{p+q}^{l'}\frac{f(E_p^l)-f(E_{p+q}^{l'})}{i\omega_n+E_p^l-E_{p+q}^{l'}},$$

$$\chi_{22}^0=+\sum_{kll'}[G_{2R}]_k^l[G_{2R}]_{k+q}^{l'}\frac{f(E_k^l)-f(E_{k+q}^{l'})}{i\omega_n+E_k^l-E_{k+q}^{l'}},$$

$$\chi_{23}^0=-\sum_{kll'}[\Gamma]_k^l[G_{2R}]_{k+q}^{l'}\frac{f(E_k^l)-f(E_{k+q}^{l'})}{i\omega_n+E_k^l-E_{k+q}^{l'}},$$

$$\chi_{24}^0=-\sum_{kll'}[G_{2R}]_k^l[\Gamma]_{k+q}^{l'}\frac{f(E_k^l)-f(E_{k+q}^{l'})}{i\omega_n+E_k^l-E_{k+q}^{l'}},$$

$$\chi_{34}^0=+\sum_{kll'}[G_{2R}]_k^l[G_1]_{k+q}^{l'}\frac{f(E_k^l)-f(E_{k+q}^{l'})}{i\omega_n+E_k^l-E_{k+q}^{l'}},$$

$$\chi_{43}^0=+\sum_{kll'}[G_1]_k^l[G_{2R}]_{k+q}^{l'}\frac{f(E_k^l)-f(E_{k+q}^{l'})}{i\omega_n+E_k^l-E_{k+q}^{l'}}. \tag{A1}$$

[1] P. Fulde and R. A. Ferrell, Superconductivity in a strong spin-exchange field, Phys. Rev. **135**, A550 (1964).

[2] A. I. Larkin and Y. N. Ovchinnikov, Inhomogeneous state of superconductors, Zh. Eksp. Teor. Fiz. **47**, 1136 (1964) [Sov. Phys. JETP **20**, 762 (1965).]

[3] For reviews of the FFLO states, see, for example, R. Casalbuoni and G. Nardulli, Inhomogeneous superconductivity in condensed matter and QCD, Rev. Mod. Phys. **76**, 263 (2004); J. J. Kinnunen, J. E. Baarsma, J.-P. Martikainen and P. Törmä, The Fulde-Ferrell-Larkin-Ovchinnikov state for ultracold

fermions in lattice and harmonic potentials: A review, Rep. Prog. Phys. **81**, 046401 (2018).

[4] Y. Matsuda and H. Shimahara, Fulde-Ferrell-Larkin-Ovchinnikov state in heavy fermion superconductors, J. Phys. Soc. Jpn. **76**, 051005 (2007).

[5] H. A. Radovan, N. A. Fortune, T. P. Murphy, S. T. Hannahs, E. C. Palm, S. W. Tozer, and D. Hall, Magnetic enhancement of superconductivity from electron spin domains, Nature (London) **425**, 51 (2003).

[6] K. Gloos, R. Modler, H. Schimanski, C. D. Bredl, C. Geibel, F. Steglich, A. I. Buzdin, N. Sato, and T. Komatsubara, Possible formation of a nonuniform superconducting state in the heavy-fermion compound UPd_2Al_3, Phys. Rev. Lett. **70**, 501 (1993).

[7] A. D. Huxley, C. Paulson, O. Laborde, J. L. Tholence, D. Sanchez, A. Junod, and R. Calemczuk, Flux pinning, specific heat and magnetic properties of the laves phase superconductor $CeRu_2$, J. Phys.: Condens. Matter **5**, 7709 (1993).

[8] A. Bianchi, R. Movshovich, C. Capan, P. G. Pagliuso, and J. L. Sarrao, Possible Fulde-Ferrell-Larkin-Ovchinnikov superconducting state in $CeCoIn_5$, Phys. Rev. Lett. **91**, 187004 (2003).

[9] C. Martin, C. C. Agosta, S. W. Tozer, H. A. Radovan, E. C. Palm, T. P. Murphy, and J. L. Sarrao, Evidence for the Fulde-Ferrell-Larkin-Ovchinnikov state in $CeCoIn_5$ from penetration depth measurements, Phys. Rev. B **71**, 020503(R) (2005).

[10] M. Croitoru and A. Buzdin, In search of unambiguous evidence of the Fulde-Ferrell-Larkin-Ovchinnikov state in quasi-low-dimensional superconductors, Condens. Matter **2**, 30 (2017).

[11] Y. Liu, T. Wei, G. He, Y. Zhang, Z. Wang, and J. Wang, Pair density wave state in a monolayer high-Tc iron-based superconductor, Nature (London) **618**, 934 (2023).

[12] H. Zhao, R. Blackwell, M. Thinel, T. Handa, S. Ishida, X. Zhu, A. Iyo, H. Eisaki, A. N. Pasupathy, and K. Fujita, Smectic pair-density-wave order in $EuRbFe_4As_4$, Nature (London) **618**, 940 (2023).

[13] A. Aishwarya, J. May-Mann, A. Raghavan, L. Nie, M. Romanelli, S. Ran, S. R. Saha, J. Paglione, N. P. Butch, E. Fradkin, and V. Madhavan, Magnetic-field-sensitive charge density waves in the superconductor UTe_2, Nature (London) **618**, 928 (2023).

[14] L. Radzihovsky and D. E. Sheehy, Imbalanced Feshbach-resonant Fermi gases, Rep. Prog. Phys. **73**, 076501 (2010).

[15] X.-J. Liu, H. Hu, and P. D. Drummond, Fulde-Ferrell-Larkin-Ovchinnikov states in one-dimensional spin-polarized ultracold atomic Fermi gases, Phys. Rev. A **76**, 043605 (2007).

[16] H. Hu and X.-J. Liu, Fulde-Ferrell superfluidity in ultracold Fermi gases with Rashba spin–orbit coupling, New J. Phys. **15**, 093037 (2013).

[17] X.-J. Liu and H. Hu, Inhomogeneous Fulde-Ferrell superfluidity in spin-orbit-coupled atomic Fermi gases, Phys. Rev. A **87**, 051608(R) (2013).

[18] Z. Zheng, M. Gong, X. Zou, C. Zhang, and G. Guo, Route to observable Fulde-Ferrell-Larkin-Ovchinnikov phases in three-dimensional spin-orbit-coupled degenerate Fermi gases, Phys. Rev. A **87**, 031602(R) (2013).

[19] M. Iskin and A. L. Subaşı, Topological superfluid phases of an atomic Fermi gas with in- and out-of-plane Zeeman fields and equal Rashba-Dresselhaus spin-orbit coupling, Phys. Rev. A **87**, 063627 (2013).

[20] F. Wu, G.-C. Guo, W. Zhang, and W. Yi, Unconventional Fulde-Ferrell-Larkin-Ovchinnikov pairing states in a Fermi gas with spin-orbit coupling, Phys. Rev. A **88**, 043614 (2013).

[21] L. He, H. Hu, and X.-J. Liu, Realizing Fulde-Ferrell superfluids via a dark-state control of Feshbach resonances, Phys. Rev. Lett. **120**, 045302 (2018).

[22] I. Bloch, J. Dalibard, and W. Zwerger, Many-body physics with ultracold gases, Rev. Mod. Phys. **80**, 885 (2008).

[23] S. Giorgini, L. P. Pitaevskii, and S. Stringari, Theory of ultracold atomic Fermi gases. Rev. Mod. Phys. **80**, 1215 (2008).

[24] G. Veeravalli, E. Kuhnle, P. Dyke, and C. J. Vale, Bragg spectroscopy of a strongly interacting Fermi gas, Phys. Rev. Lett. **101**, 250403 (2008).

[25] S. Hoink, P. Dyke, M. G. Lingham, J. J. Kinnunen, G. M. Bruun and C. J. Vale, Goldstone mode and pair-breaking excitations in atomic Fermi superfluid, Nat. Phys. **13**, 943 (2017).

[26] X. Li, X. Luo, S. Wang, K. Xie, X.-P. Liu, H. Hu, Y.-A. Chen, X.-C. Yao, and J.-W. Pan, Second sound attenuation near quantum criticality, Science **375**, 528 (2022).

[27] P. Dyke, S. Musolino, H. Kurkjian, D. J. M. Ahmed-Braun, A. Pennings, I. Herrera, S. Hoinka, S. J. J. M. F. Kokkelmans, V. E. Colussi, and C. J. Vale, Higgs oscillations in a unitary Fermi superfluid, arXiv:2310.03452 [Phys. Rev. Lett. (to be published)].

[28] R. Senaratne, D. C.-Cavazos, S. Wang, F. He, Y.-T. Chang, A. Kafle, H. Pu, X.-W. Guan, and R. G. Hulet, Spin-charge separation in a one-dimensional Fermi gas with tunable interactions, Science **376**, 1305 (2022).

[29] J. Y. Lee and X. W. Guan, Asymptotic correlation functions and FFLO signature for the one-dimensional attractive spin-1/2 Fermi gas, Nucl. Phys. B **853**, 125 (2011).

[30] P. W. Anderson, Random-phase approximation in the superconductivity, Phys. Rev. **112**, 1900 (1958).

[31] X.-J. Liu, H. Hu, A. Minguzzi, and M. P. Tosi, Collective oscillations of a confined Bose gas at finite temperature in the random-phase approximation, Phys. Rev. A **69**, 043605 (2004).

[32] L. He, Dynamic density and spin responses of a superfluid Fermi gas in the BCS-BEC crossover: Path integral formulation and pair fluctuation theory, Ann. Phys. **373**, 470 (2016).

[33] P. Zou, E. D. Kuhnle, C. J. Vale, and H. Hu, Quantitative comparison between theoretical predictions and experimental results for Bragg spectroscopy of a strongly interacting Fermi superfluid, Phys. Rev. A **82**, 061605(R) (2010).

[34] P. Zou, H. Hu, and X.-J. Liu, Low-momentum dynamic structure factor of a strongly interacting Fermi gas at finite temperature: The Goldstone phonon and its Landau damping, Phys. Rev. A **98**, 011602(R) (2018).

[35] H. Biss, L. Sobirey, N. Luick, M. Bohlen, J. J. Kinnunen, G. M. Bruun, T. Lompe, and H. Moritz, Excitation spectrum and superfluid gap of an ultracold Fermi gas, Phys. Rev. Lett. **128**, 100401 (2022).

[36] H. Zhao, X. Gao, W. Liang, P. Zou and F. Yuan, Dynamical structure factors of a two-dimensional Fermi superfluid within random phase approximation, New J. Phys. **22**, 093012 (2020).

[37] K. Yang, Inhomogeneous superconducting state in quasi-one-dimensional systems, Phys. Rev. B **63**, 140511(R) (2001).

[38] Z. Gao, L. He, H. Zhao, S.-G. Peng, and P. Zou, Dynamic structure factor of one-dimensional Fermi superfluid with spin-orbit coupling, Phys. Rev. A **107**, 013304 (2023).

[39] H. Zhao, X. Yan, S.-G. Peng, and P. Zou, Dynamic structure factor of two-dimensional Fermi superfluid with Rashba spin-orbit coupling, Phys. Rev. A **108**, 033309 (2023).
[40] J. M. Edge and N. R. Cooper, Signature of the Fulde-Ferrell-Larkin-Ovchinnikov phase in the collective modes of a trapped ultracold Fermi gas, Phys. Rev. Lett. **103**, 065301 (2009).
[41] M. O. J. Heikkinen and P. Törmä, Collective modes and the speed of sound in the Fulde-Ferrell-Larkin-Ovchinnikov state, Phys. Rev. A **83**, 053630 (2011).
[42] K. V. Samokhin, Goldstone modes in Larkin-Ovchinnikov-Fulde-Ferrell superconductors, Phys. Rev. B **81**, 224507 (2010).
[43] Z. Huang, C. S. Ting, J.-X. Zhu, and S.-Z. Lin, Gapless Higgs mode in the Fulde-Ferrell-Larkin-Ovchinnikov state of a superconductor, Phys. Rev. B **105**, 014502 (2022).
[44] H. Zhao, P. Zou, and F. Yuan, Dynamical structure factor and a new method to measure the pairing gap in two-dimensional attractive Fermi-Hubbard model, arXiv:2305.09685.
[45] H. Zhao, R. Han, L. Qin, F. Yuan, and P. Zou, A universal pairing gap measurement proposal by dynamical excitations in 2D doped attractive Fermi-Hubbard model with spin-orbit coupling, arXiv:2401.17488.